

Original Article

Open Access



A comparison study to detect seam carving forgery in JPEG images with deep learning models

Naciye Hafsa Celebi¹, Tze-Li Hsu², Qingzhong Liu¹

¹Department of Computer Science, Sam Houston State University, Huntsville, TX 77341, USA.

²Department of Sociology, Sam Houston State University, Huntsville, TX 77341, USA.

Correspondence to: Prof./Dr. Qingzhong Liu, Department of Computer Science, Sam Houston State University, Huntsville, TX 77341, USA. E-mail: liu@shsu.edu

How to cite this article: Celebi NH, Hsu TL, Liu QZ. A comparison study to detect seam carving forgery in JPEG images with deep learning models. *J Surveill Secur Saf* 2022;3:88-100. <http://dx.doi.org/10.20517/jsss.2022.02>

Received: 17 Jan 2022 **First Decision:** 19 May 2022 **Revised:** 16 Aug 2022 **Accepted:** 19 Aug 2022 **Published:** 24 Aug 2022

Academic Editors: Khan Muhammad, Xiangyang Luo **Copy Editor:** Haixia Wang **Production Editor:** Haixia Wang

Abstract

Aim: Although deep learning has been applied in image forgery detection, to our knowledge, it still falls short of a comprehensive comparison study in detecting seam-carving images in multimedia forensics by comparing the popular deep learning models, which is addressed in this study.

Methods: To investigate the performance in detecting seam-carving-based image forgery with popular deep learning models that were used in image forensics, we compared nine different deep learning models in detecting untouched JPEG images, seam-insertion images, and seam removal images (three-class classification), and in distinguishing modified seam-carving images from untouched JPEG images (binary classification). We also investigate the different learning algorithms with the Efficientnet-B5 in adjusting the learning rate with three popular optimizers in deep learning.

Results: Our study shows that EfficientNet performs the best among the nine different deep learning frameworks, followed by SRnet, and Lfnet. Different algorithms for adjusting the learning rate result in different detection testing accuracy with Efficientnet-B5. In our experiments, decouples the optimal choice of weight decay factor from the setting of the learning rate (AdamW) is generally superior to Adaptive Moment Estimation (Adam) and Stochastic Gradient Descent (SGD). Our study also indicates that deep learning is very promising for image forensics, such as the detection of image forgery.



© The Author(s) 2022. **Open Access** This article is licensed under a Creative Commons Attribution 4.0 International License (<https://creativecommons.org/licenses/by/4.0/>), which permits unrestricted use, sharing, adaptation, distribution and reproduction in any medium or format, for any purpose, even commercially, as long as you give appropriate credit to the original author(s) and the source, provide a link to the Creative Commons license, and indicate if changes were made.



Conclusion: Deep learning is very promising in image forensics that is hardly discernable to human perceptions, but the performance varies over different learning models and frameworks. In addition to the models, the optimizer has a considerable impact on the final detection performance. We would recommend EfficientNet, Lfnet and SRnet for seam-carving detection.

Keywords: Seam carving, convolutional neural network, deep learning, EfficientNet, SRnet, Lfnet, AdamW, Adam, SGD, image forensics

INTRODUCTION

Digital images have played an essential role in our daily lives. Digital image editing tools are easily available and have evolved tremendously due to the increasing requests. With the popularity of open-source image editing tools that are easily accessible, many individuals without advanced image processing techniques can effortlessly generate a fake image. Hence, the authenticity of the images in the virtual environment becomes a critical problem [1,2].

Seam carving is one of the popular image manipulation strategies adequate for content-aware image resizing. The functionality of seam carving is to assemble several seams in an image and automatically eliminate seams to decrease image size or insert seams to extend it. The corresponding image is reduced by one pixel in height/width at a time. In seam carving, the idea is that the given input image is resized by removing or inserting optimal seams described as corresponding pixel paths reaching from top to bottom or left to right while keeping the photorealism of the image. The seam located vertically in an image is a path of pixels linked with one pixel per row from top to bottom. The seam located horizontally is a way of pixels linked from left to right with one pixel per column. Hence, the underlying algorithm is elegant and straightforward. By reducing the energy cost of a seam [3,4] to re-generate an image, seam carving can efficiently resize an image [5]. By using seam carving, an unwanted object can be removed from an image without any perceivable distortion [6,7].

As mentioned, seam carving has been applied for object removal and image resizing; it is also applied for tampering with illusions such as image or object insertion in image. Seam carved images can be intentionally manipulated to misinterpret or extract original content in the image; thus, detecting the forgery content, which are artifacts of seam carving, has evolved into a crucial issue in multimedia forensics [8,9].

In image forensics, many methods have been proposed to detect image steganography and image forgery, including but not limited to the detection of seam carving. These methods may potentially be applied to the detection of seam carving forgery. These works contain the detection of distinct image manipulations such as morphing [10,11], resampling [12,13], splicing [14,15], copy-move [16,17], seam carving [18,19], and inpainting based-object removal [20,21]. Some approaches also exploit JPEG blocking artifacts to detect tampered regions [22,23], while more recent research exploits deep learning-based methods [24-26].

RELATED WORK

Introduction to seam carving

In seam carving, imperceptible pixels on the least essential seams coordinating with their surroundings are terminated or inserted to perform content-aware scaling. Formally, let I will be a $p \times q$ image, and a vertical seam is defined by:

$$S^X = \{S_i^x\}_{i=1}^p = \{(x(i), i)\}_{i=1}^p \quad (1)$$

where x is a mapping $x: [1, \dots, p] \times [1, \dots, q]$.

Similarly, a horizontal seam is defined by:

$$S^Y = \left\{ s_j^y \right\}_{j=1}^q = \{(j, y(j))\}_{j=1}^q \tag{2}$$

$$\text{s.t. } \forall j, |y(j) - y(j - 1)| \leq 1$$

where y is a mapping $y: [1, \dots, q] \times [1, \dots, p]$.

The pixel path of seam S is denoted as I_S . Given an energy function e , the cost of a seam is calculated by $E(S) = E(I_S) = \sum_{i=1}^p e(I(S_i))$. The optimal seam S^* generally minimizes the seam cost:

$$S^* = \min_S E(S) = \min_S \sum_{i=1}^p e(I(S_i)) \tag{3}$$

In the reference^[4], several image importance measures are examined as the energy function. Although no single energy function performs well across all images, in general, the following two measures e_1 and e_{HoG} work quite well.

$$e_1(I) = \left| \frac{\partial}{\partial x} I \right| + \left| \frac{\partial}{\partial y} I \right| \tag{4}$$

$$e_{HoG}(I) = \frac{\left| \frac{\partial}{\partial x} I \right| + \left| \frac{\partial}{\partial y} I \right|}{(HoG(I(x, y)))} \tag{5}$$

where $HoG(I(x, y))$ is a histogram of oriented gradients at each pixel.

Seam carving and relevant image forgery detection

Sarker et al.^[5] proposed a blind seam carving detection system which models the distinction JPEG 2-D array with Markov random process^[27]; in their detection system, the Markov features are utilized to exhibit the imprint in block-based frequency-domain to distinguish modified images from original ones. Fillion and Sharma^[28] proposed a model comprising energy bias-based features and decisive wavelet moments to detect seam carving. Chang et al.^[29] illustrated the artifact caused by seam carving in JPEG images. They discussed the misalignment due to the modification occurrence, and seam-carved images and unaltered images may have distinctive DCT blocking artifacts when recompression has been made^[30]. Liu et al.^[7] proposed rich model-based features^[31] with calibrated neighboring joint density and a hybrid large feature mining approach to achieve state-of-the-art in terms of detection accuracy^[32]. Deep learning is widely used for various areas^[33-39], it is also applied to detect image forgery^[40-42]. For example, Yao et al.^[43] developed a reliability fusion map based CNN model to detect image forgery. Du et al.^[44] proposed a locality-aware autoencoder to detect deepfake images. The authors used a pixel-wise mask to regularize the local interpretation of Locality-Aware AutoEncoders to improve the model’s generalization capabilities. The authors evaluated their proposed approach on the Dresden dataset. They claimed that their model achieved high performance. Thakur et al.^[45] proposed two algorithms to classify and localize image forgery. The authors evaluated their proposed approach

using the CASIA-v1, CASIA-v2, DVMM, and BSDS300 datasets. They reported that their proposed approach achieved state-of-the-art performance. Majumder *et al.* [42] developed a CNN architecture to train a model for forgery detection. The researchers tested their solution on the CASIA v2 dataset. They also applied transfer learning to adapt VGG-16, VGG-19, and Resnet models for forgery detection. The authors compared the performance of their proposed model with the transfer learning models. Their method achieved good performance without multi-level feature extraction, and that transfer learning is unsuitable for this task. Muhammad *et al.* [46] developed an image forgery detection method based on the steerable pyramid transform and local binary pattern techniques. Their proposed method was evaluated on three datasets: CASIA v1, CASIA v2, and Columbia color image. Goel *et al.* [47] developed a copy move forgery detection algorithm that uses dual branch convolutional neural networks to identify forged images. Le-Tien *et al.* [48] developed a technique to identify forged images using neural networks. The authors evaluated their model on the CASIA-v2 dataset. Diallo *et al.* [41] developed a framework for deep learning detection of forged images. The researchers evaluated their proposed framework on the CMI dataset. They also evaluated a set of transfer learning models adapted to forgery detection, namely, ResNet, VGG-19, and DenseNet. Han *et al.* [49] applied Maximum Mean Discrepancy (MMD) loss to train a machine learning model for forgery detection. The authors evaluated their proposed approach on the DF-TIMIT, UADFV, Celeb-DF, and FaceForensics++ datasets. Aneja *et al.* [50] developed a new transfer learning approach for forgery detection. The authors evaluated their approach on the FaceForensics++ dataset. Bourouis *et al.* [51] developed a framework for the Bayesian learning of finite GID mixture models. The authors evaluated their approach using forgery detection. The datasets used are MICC-F220 and MICC-F2000. Cao *et al.* [52] developed an anti-compression facial forgery detection technique which extracts compression insensitive features from compressed and uncompressed forgeries and learns a robust partition. Asghar *et al.* [53] developed an image forensics technique that uses discriminative robust local binary patterns to encode tamper traces. Their approach also uses an SVM classifier to detect forged images. Zhang *et al.* [54] applied a cross-layer intersection mechanism to a dense u-net classifier for image forgery detection. They evaluated their approach on several datasets: CASIA, NC2016, and Columbia Uncompressed. Optimization needs to be performed during detections [55–58]. Other seam-carving-based detection includes but not limited to [59–62].

Deep learning model-based approaches are widely applied for image forgery detection. These techniques can improve different aspects of life and research on image forgery detection is required. Unfortunately, it falls short of a comprehensive comparison of the state-of-the-art deep learning models in detection image forgery, especially seam-carving image forgery in JPEG images, which is addressed by our study.

METHODS

Dataset

The dataset used in this research is a custom-balanced dataset. The dataset contains 12916 images. Half of the dataset, 6458 images, are untouched JPEG images and the rest of 6458 were touched images (altered/manipulated) using seam carving with a quality of 75. The untouched images are everyday pictures of dimensions 1234×1858 or 1858×1234 . Touched images are modified by removed objects, horizontal and/or vertical resizing or other forms of image forgery. Figure 1 represents examples of the images from the dataset. In the touch images category, some of the modifications can be easily observed with the human eye; on the other hand, some of them have subtle signal modifications which cannot be distinguished by the human eye and are visually perceptible. In our experiment, images that were exclusively resizing the original image are not considered and not included in the dataset. In other words, we exclude the dimensional modified images in the untouched image set. Therefore, excluding resized images from the untouched set eliminates the vagueness in labeling when we resize the images. Our model constrained us to train on smaller resized versions of the image. Excluding resized images from our dataset eliminates the ambiguity in labeling when we resize our images for uniformity. Figure 1 shows untouched image examples on the left and doctored image examples by seam carving on the



Figure 1. Examples of untouched (on the left) and seam-carving (on the right) in JPEG image.

right.

CNN Architecture

Figure 2 briefly shows the architecture of a simple convolutional neural network (CNN), which starts with an input dataset that mainly combines images and videos. The convolutional layer is the first step of the CNN structure that takes the input images and extracts various features. In this layer, convolution operations are conducted within the input and a filter. The output received after applying the convolutional layer is a feature map with some activation functions. The taken feature map is then fed to other layers to comprehend various other features of the input image. In most CNN architectures, the pooling layer is the next step after the convolutional layer. The pooling layer performs by decreasing the connections between layers and independently operates on the feature map to reduce the computational costs. The Pooling Layer is used as a bridge between the Convolutional Layer and the Fully Connected Layer. After the Pooling layer, the output layers are flattened and fed to the Fully connected layer — this layer is based on weights and biases and the neurons. The Fully Connected layer is used to connect the neurons between two different layers, and these layers are the last layers of the CNN structure. It is worthy of noting that Figure 2 only shows a simple architecture of a CNN, and different deep learning models come out with different structures and different layers.

CNN has shown tremendous success in image processing and computer vision. CNN works typically by a number of convolutional layers chained together with fully connected layers. Using two-dimensional filters, CNN computes the feature map of the given image. The layers also include max-pooling layers, which preserve significant features of the image. In CNN, the output of the last convolutional layer is kept by the dense layer by converting the layer to a vector; in other words, the last layer is converted to a vector by flattening the layer. Then softmax function is used in the dense layer by multiclass classification. Multiclass classification specifies probability values for each class.

EfficientNet architecture

Tan and Le proposed a model called EfficientNet^[59]. In their research, they expanded CNN architecture by scaling models. To improve CNN architecture performance, scaling in resolution, depth, and width is required. The most common way to scale up CNN architecture was either by one of the three dimensions: depth, width, or image resolution. On the other hand, EfficientNets perform compound scaling, which scales all three dimensions while preserving a balance between all network dimensions. Compound scaling is also used on ResNet architectures. Usually, the dimensions are tested arbitrarily to improve model accuracy in

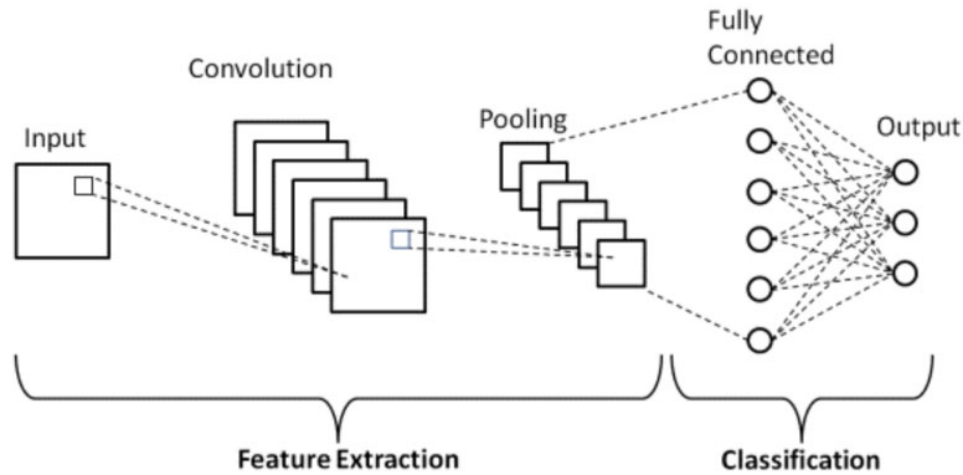


Figure 2. A simple CNN Architecture.

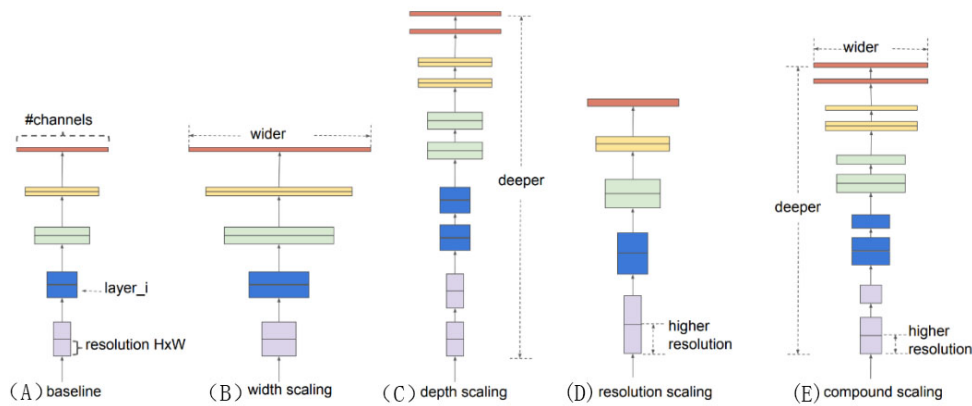


Figure 3. Model scaling in EfficientNet [59].

practice. The authors adopted the more principled approach to scaling the model on every dimension using fixed scaling coefficients. Whenever the fixed scaling coefficients are determined, the black-box networks are scaled to reach higher accuracy. In this study, EfficientNet is represented by three dimensions: (1) depth; (2) width; and (3) resolutions; the parameter scales by every dimension as a σ .

- (1) depth = α^σ
- (2) width = β^σ
- (3) resolution = γ^σ

$$s * t * \alpha * \beta^2 * \gamma^2 \approx 2 \tag{6}$$

$$\alpha \geq 1, \beta \geq 1, \gamma \geq 1$$

where are obtained by using grid search. This equation provides a balance between computation cost and performance. Figure 3 shows the architecture model scaling in the study [59].

Starting from the baseline EfficientNet-B0, the authors in the paper [59] apply the compound scaling method to scale it up with two steps:

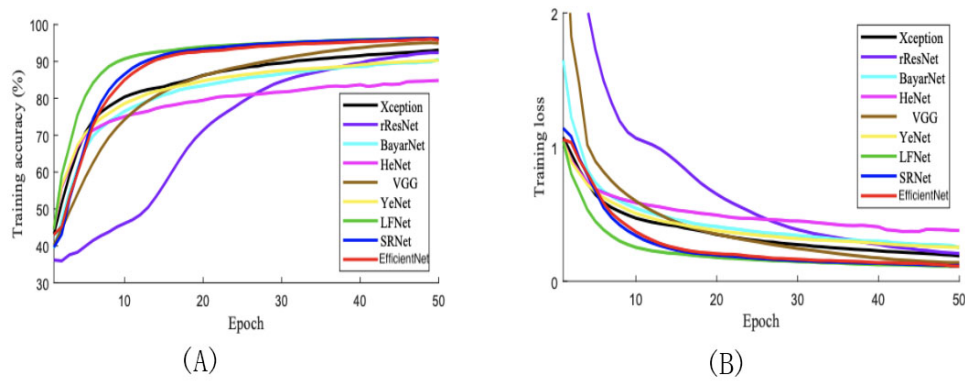


Figure 4. (A) Training accuracy and training loss (B) tendencies for each network for 50 epochs.

STEP 1: first fix $\sigma = 1$, assuming twice more resources available, and do a small grid search of α, β, γ . In particular, the best values for EfficientNet-B0 are $\alpha = 1.2, \beta = 1.1, \gamma = 1.15$, under constraint of $\alpha * \beta^2 * \gamma^2 \approx 2$.

STEP 2: then fix α, β, γ as constants and scale up baseline network with different σ , to obtain EfficientNet-B1 to B7.

We compare AlexNet^[63], Xception^[64], ResNet50^[33], VGG^[34], BayarNet^[35], HeNet^[36], YeNet^[37], LFNNet^[38], SRNet^[39] and EfficientNet^[59] models in our experiment. These models are slightly modified to make three predicted probabilities in the last layer. In the experiment, each model was trained until it was adequately incorporated in terms of training accuracy and loss for 50 epochs. Figure 4 shows the training accuracy (A) and training loss (B) for each network for 50 epochs.

The learning scheduler ReduceLROnPlateau^[58] is used to allow dynamic learning rate reduction based on some validation measurements. The scheduler had a factor of 0.5, a patience value of 1, and a threshold of 0.0001. The cross-entropy loss is adopted. Cross-entropy for n-classes is defined as

$$L_{CE} = - \sum_{i=1}^n t_i \log(p_i) \tag{7}$$

Where t_i is the truth label and p_i is the softmax probability for the i^{th} class,

$$p(z)_i = \frac{e^{z_i}}{\sum_{j=1}^n e^{z_j}} \tag{8}$$

The experiment shows that trivial progress appeared in the implementation of each model after 50 epochs. We utilized multiple classifiers in the experiments.

Evaluation metrics

In this research, evaluation of classification accuracy is measured, which is $(nt/ts)100(\%)$, where nt represents the total number of correctly predicted values and ts represents the total number of testing samples. While original and seam-insertion images were classified (the latter two are produced based on original untouched images), each class’s ratio data was possessed at 1:1:1 when calculating the testing set. In addition, the receiver operating characteristic (ROC) curves were calculated to assess the performance of all the Deep Learning

Table 1. Performance evaluation of CNN models (%)

Ratio	Xception	ResNet	BayarNet	HeNet	VGG	YeNet	LFNet	SRNet	EfficientNet
10%	67.34	74.43	65.73	65.48	76.23	78.12	89.26	87.56	89.12
20%	78.45	80.51	81.87	81.76	85.32	85.32	95.32	95.76	95.33
30%	87.67	88.34	88.23	88.42	93.29	93.29	98.12	98.34	98.67
40%	90.67	90.23	93.42	92.73	95.76	95.76	98.43	99.41	99.53
50%	93.43	93.90	94.92	93.34	95.64	95.64	98.79	99.87	99.67
Mixed	84.12	86.07	85.78	84.87	89.43	89.43	96.78	96.48	98.13

models. The area under AUC curve is used as a performance evaluation and the ROC curve is used to represent the relation between the true positive rate and the false positive rate. If the value of AUC is close to 1, it is considered as the model has outstanding performance, which also means it has a good measure of separability.

Performance evaluation of networks

In the performance of evaluation, we first evaluated the performance of EfficientNet and compared it with other CNNs. Table 1 shows the result of retargeting ratio parameters. The end of the table represents the classification results for a mixed test set for the sets that include 10% to 50% retargeting ratio. The accuracy values of EfficientNet for a 10% to 50% retargeting ratio are 89.12%, 98.33%, 98.67%, 99.53%, and 99.67%, respectively. The EfficientNet's classification performance in the mixed set is 98.13% which has the highest accuracy received in all CNN-based models, followed by LFNet and SRnet, which also shows excellent performance for seam-carving detection in the JPEG domains.

An AUC ROC is used for visualizing a model's performance between sensitivity and specificity. Sensitivity refers to the ability to correctly identify entries that fall into the positive class. On the other hand, specificity refers to the ability to correctly identify entries that fall into the negative class. Hence, an AUC ROC plot is used to identify how well the model can distinguish between classes. In our experiment, we performed three class classifications which represent original, seam inserted, and seam removed. To distinguish the images among the three classes: original (class 0), seam inserted (class 1), and seam removed (class 2), the ROC curve for each class was generated, and each AUC value for the ROC curves was calculated. For every CNN model, we instantiate a visualizer object and fit that to the training data, then generate the score by feeding in the test data.

Figure 5 illustrates the ROC curves that were computed to evaluate the performance of CNN models in detail. As illustrated in Figure 5, the ROC curve for three class generation was performed, and each AUC value for the ROC curves was calculated. ROC curves of EfficientNet, LFNet, and SRNet measurements were closer to each other, and we can conclude that EfficientNet, LFNet, and SRNet perform better than the other CNN models. The AUC values with EfficientNet are 0.991, 0.996, and 0.994 for each class, which are higher than the ones with LFNet and SRNet. The thoroughly analyzed results of Table I and Figure 5 reveal that the EfficientNet performs the best.

We also compared the three popular optimizers: Stochastic Gradient Descent (SGD)^[55], Adam (Adaptive Moment Estimation)^[56], and decouples the optimal choice of weight decay factor from the setting of the learning rate for Adam (AdamW)^[57] in the binary classification between untouched JPEG images and seam-carving JPEG images.

Adaptive optimizers like Adam have become a default choice for training neural networks. However, when aiming for state-of-the-art results, researchers often prefer stochastic gradient descent (SGD) with momentum because models trained with Adam have been observed not to generalize as well.

Weight decay is performed only after controlling the parameter-wise step size in Adam optimizer. The weight

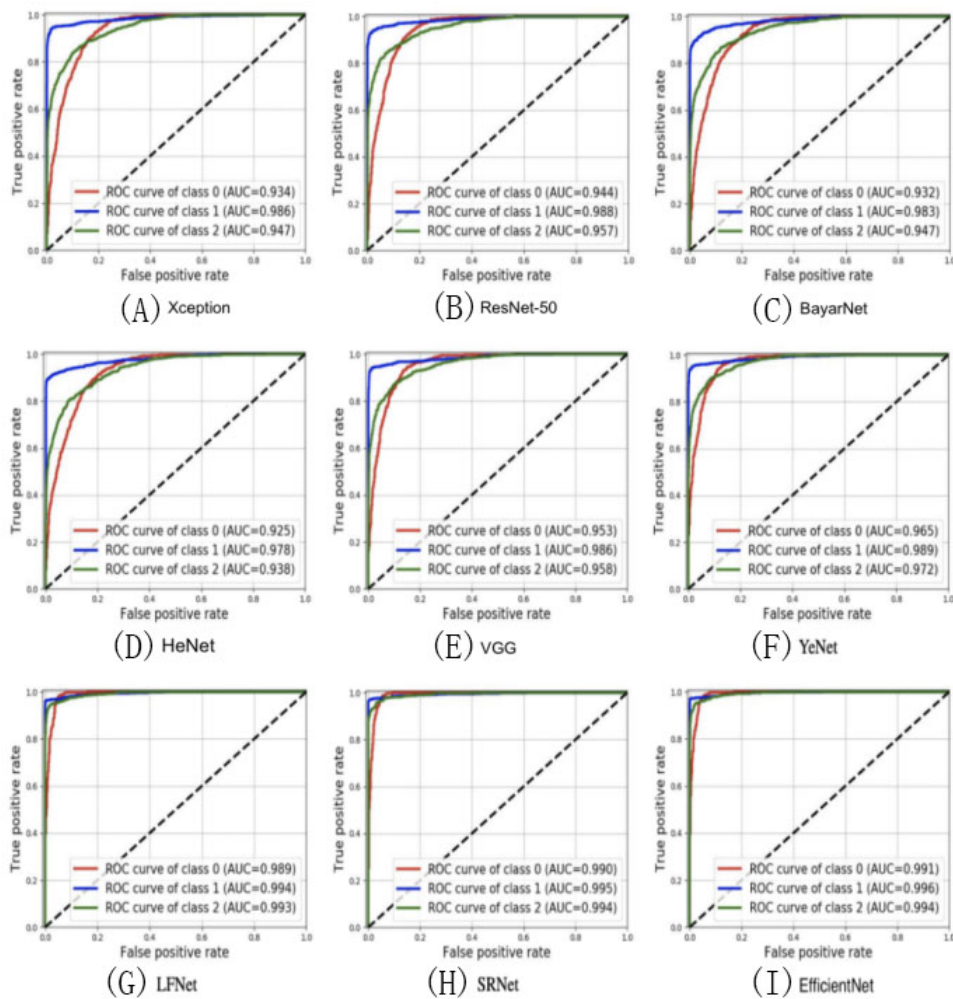


Figure 5. The ROC curve for three class generation was performed, which represents original, seam inserted, and seam removed. To distinguish the images among the three classes: original (class 0), seam inserted (class 1), and seam removed (class 2), each AUC value for the ROC curves was calculated.

decay or regularization term does not end up in the moving averages and is thus only proportional to the weight itself. The authors^[57] show experimentally that AdamW yields better training loss and that the models generalize much better than models trained with Adam.

We compare Adam, AdamW, and SGD optimizers in this study. We ran ten experiments under each learning algorithm with randomly selected training data set, validation dataset, and testing dataset on each experiment, the boxplots of the ten testing results under the three optimizers are given in Figure 6. The X-axis shows the three groups of optimizers, and Y-axis shows the testing accuracy (%). Our results show that the AdamW and Adam are better than SGD in this study.

We would note that AdamW and Adam perform better than SGD with EfficientNet-B5 in this study, while across different deep learning architectures and different deep learning models in a recent study in detecting COVID-19 chest X-ray images, SGD is generally superior to Adam and AdamW^[26].

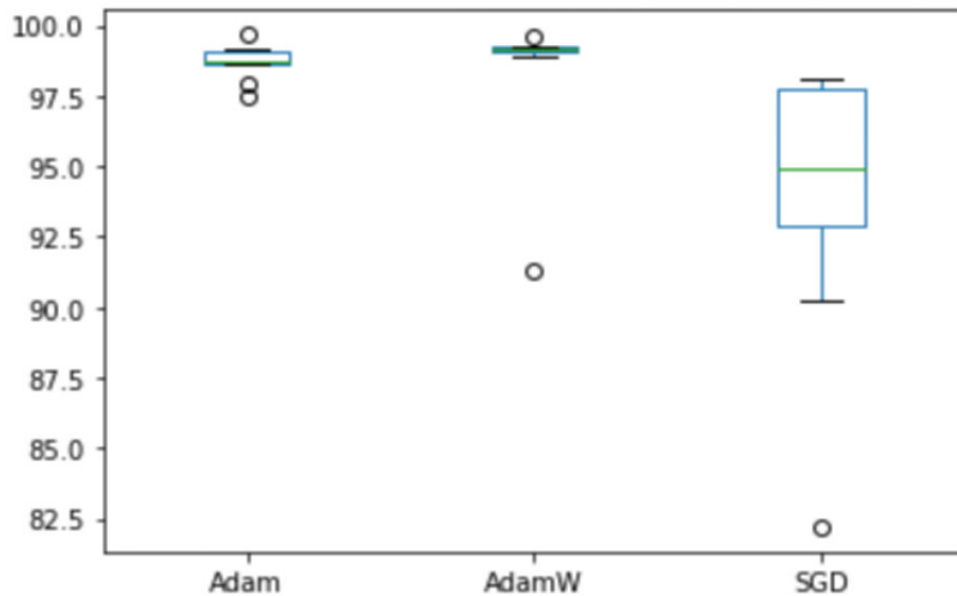


Figure 6. Boxplots of three learning algorithms with EfficientNet-B5.

RESULTS

Deep learning is very successful in computer vision, e.g., object detection, image classification, but these tasks can be easily perceived by human beings. However, it is incapable for human eyes to distinguish forged images from untouched ones. To investigate the performance in detecting seam-carving-based image forgery with popular deep learning models that were used in image forensics, including image steganalysis and image forgery detection, we compared several deep learning models, and the study shows that EfficientNet performs the best, followed by SRnet and LFnet. The current study also demonstrates that the different optimizers led to different detection testing accuracy with the Efficientnet-B5. In the experiments, AdamW is generally superior to Adam and SGD. The current study also indicates that deep learning is very promising in image forensics that is hardly discernable to human perceptions.

DECLARATIONS

Authors' contributions

Performed the comparison study of the nine deep learning models and drafted the paper: Celebi NH
Helped in producing a part of the data and assisted in the draft: Hsu TL
Supervised the study, assisted in the experiments, and the draft: Liu QZ

Availability of data and materials

Dataset will be availables at https://github.com/Frank-SHSU/seam_carving-image-dataset

Financial support and sponsorship

None.

Conflicts of interest

All authors declared that there are no conflicts of interest.

Ethical approval and consent to participate

Not applicable.

Consent for publication

Not applicable.

Copyright

© The Author(s) 2022.

REFERENCES

1. Birajdar GK, Mankar VH. Digital image forgery detection using passive techniques: a survey. *Digital Investigation* 2013;10:226-45. DOI
2. Qureshi MA, Deriche M. A bibliography of pixel-based blind image forgery detection techniques. *Signal Processing: Image Communication* 2015;39:46-74. DOI
3. Ke Y, Shan Q, Qin F, Min W, Guo J. Detection of seam carved image based on additional seam carving behavior. *IJSIP* 2016;9:167-78. DOI
4. Avidan S, Shamir A. Seam carving for content-aware image resizing. *ACM Trans Graph* 2007;26:10. DOI
5. Sarkar A, Nataraj L, Manjunath BS. Detection of seam carving and localization of seam insertions in digital images, Proc. 11th ACM Workshop on Multimedia and Security (MM&Sec'09), NY, USA, pp. 107-116, 2009.
6. Yin T, Yang G, Li L, Zhang D, Sun X. Detecting seam carving based image resizing using local binary patterns. *Computers & Security* 2015;55:130-41. DOI
7. Liu Q. An approach to detecting JPEG down-recompression and seam carving forgery under recompression anti-forensics. *Pattern Recognition* 2017;65:35-46. DOI
8. Lu M, Niu S. Detection of image seam carving using a novel pattern. *Comput Intell Neurosci* 2019;2019:9492358. DOI PubMed PMC
9. SSeam carving based image resizing detection using hybrid features. *Teh vjesn* 2017;24. DOI
10. Jassim S, Asaad A. Automatic detection of image morphing by topology-based analysis. In 2018 26th European Signal Processing Conference (EUSIPCO), pages 1007–1011. IEEE, 2018.
11. Neubert T. Face Morphing Detection: An Approach Based on Image Degradation Analysis. In: Kraetzer C, Shi Y, Dittmann J, Kim HJ, editors. *Digital Forensics and Watermarking*. Cham: Springer International Publishing; 2017. pp. 93-106. DOI
12. Popescu A, Farid H. Exposing digital forgeries by detecting traces of resampling. *IEEE Trans Signal Process* 2005;53:758-67. DOI
13. Ryu S, Lee H. Estimation of linear transformation by analyzing the periodicity of interpolation. *Pattern Recognition Letters* 2014;36:89-99. DOI
14. Guillemot C, Le Meur O. Image inpainting : overview and recent advances. *IEEE Signal Process Mag* 2014;31:127-44. DOI
15. Salloum R, Ren Y, Jay Kuo C. Image Splicing Localization using a Multi-task Fully Convolutional Network (MFCN). *Journal of Visual Communication and Image Representation* 2018;51:201-9. DOI
16. Cozzolino D, Poggi G, Verdoliva L. Efficient Dense-Field Copy-Move Forgery Detection. *IEEE Trans Inform Forensic Secur* 2015;10:2284-97. DOI
17. Jian Li, Xiaolong Li, Bin Yang, Xingming Sun. Segmentation-based image copy-move forgery detection scheme. *IEEE Trans Inform Forensic Secur* 2015;10:507-18. DOI
18. Gong Q, Shan Q, Ke Y, Guo J. Detecting the location of seam and recovering image for seam inserted image. *JCM* 2018;18:499-509. DOI
19. Li Y, Xia M, Liu X, Yang G. Identification of various image retargeting techniques using hybrid features. *Journal of Information Security and Applications* 2020;51:102459. DOI
20. Liang Z, Yang G, Ding X, Li L. An efficient forgery detection algorithm for object removal by exemplar-based image inpainting. *Journal of Visual Communication and Image Representation* 2015;30:75-85. DOI
21. Wu Q, Sun SJ, Zhu W, Li GH, Tu D. Detection of digital doctoring in exemplar-based inpainted images. In *Machine Learning and Cybernetics, 2008 International Conference on*. 2008;3:1222-6. DOI
22. Farid H. Exposing Digital Forgeries From JPEG Ghosts. *IEEE Trans Inform Forensic Secur* 2009;4:154-60. DOI
23. Luo W, Huang J, Qiu G. JPEG Error Analysis and Its Applications to Digital Image Forensics. *IEEE Trans Inform Forensic Secur* 2010;5:480-91. DOI
24. Bayar B, Stamm MC. A deep learning approach to universal image manipulation detection using a new convolutional layer. In *Proceedings of the 4th ACM Workshop on Information Hiding and Multimedia Security*. 2016:5-10. DOI
25. Rao Y, Ni JQ. A deep learning approach to detection of splicing and copy-move forgeries in images. In *Information Forensics and Security (WIFS), International Workshop on*. 2016:1–6. DOI
26. Liu Q, Chen Z, Liu HC. A comparison study to detect COVID-19 X-ray images with SOTA deep learning models. *Proceedings of the 1st Workshop on Healthcare AI and COVID-19. ICML 2022*;184:146-153. DOI
27. Shi YQ, Chen C, Chen W. A Markov Process Based Approach to Effective Attacking JPEG Steganography. In: Camenisch JL, Collberg CS, Johnson NF, Sallee P, editors. *Information Hiding*. Berlin: Springer Berlin Heidelberg; 2007. pp. 249-64. DOI
28. Fillion C, Sharma G. Detecting content adaptive scaling of images for forensic applications. *Media Forensics and Security, SPIE Proc.*, p. 75410, 2010. DOI
29. Chang W, Shih TK, Hsu H. Detection of seam carving in JPEG images. in: *Proceedings of the 2013 International Joint Conference on Awareness Science and Technology and Ubi-media Computing*, pp 632-638, 2013. DOI
30. Wattanachote K, Shih TK, Chang W, Chang H. Tamper Detection of JPEG Image Due to Seam Modifications. *IEEE Trans Inform Forensic*

- Secur* 2015;10:2477-91. DOI
31. Fridrich J, Kodovsky J. Rich models for steganalysis of digital images. *IEEE Trans Inform Forensic Secur* 2012;7:868-82. DOI
 32. Liu Q. Exposing seam carving forgery under recompression attacks by hybrid large feature mining. 23rd Int. Conf. on Pattern Recog. (ICPR), pp. 1036-1041, 2016. DOI
 33. He K, Zhang X, Ren S, Sun J. Deep residual learning for image recognition. 2016 IEEE Conference on Computer Vision and Pattern Recognition (CVPR), 2016:770-778. DOI
 34. Nam SH, Park J, Kim D, Yu IJ, Kim TY, Lee HK. Two stream network for detecting double compression of h. 264 videos, in 2019 IEEE International Conference on Image Processing (ICIP). IEEE, 2019, pp. 111–115. DOI
 35. Gallucci M. At last, wave energy tech plugs into the grid - [News]. *IEEE Spectr* 2019;56:8-9. DOI
 36. He P, Jiang X, Sun T, Wang S, Li B, Dong Y. Frame-wise detection of relocated I-frames in double compressed H.264 videos based on convolutional neural network. *Journal of Visual Communication and Image Representation* 2017;48:149-58. DOI
 37. Ye J, Shi Y, Xu G, Shi Y. A Convolutional Neural Network Based Seam Carving Detection Scheme for Uncompressed Digital Images. In: Yoo CD, Shi Y, Kim HJ, Piva A, Kim G, editors. *Digital Forensics and Watermarking*. Cham: Springer International Publishing; 2019. pp. 3-13. DOI
 38. Ono Y, Trulls E, Fua PV, Yi KM. (2018). LF-Net: Learning Local Features from Images. ArXiv, abs/1805.09662. DOI
 39. Boroumand M, Chen M, Fridrich J. Deep Residual Network for Steganalysis of Digital Images. *IEEE Trans Inform Forensic Secur* 2019;14:1181-93. DOI
 40. Liu Q. An Improved Approach to Exposing JPEG Seam Carving Under Recompression. *IEEE Trans Circuits Syst Video Technol* 2019;29:1907-18. DOI
 41. Diallo B, Urruty T, Bourdon P, Fernandez-maloigne C. Robust forgery detection for compressed images using CNN supervision. *Forensic Science International: Reports* 2020;2:100112. DOI
 42. Majumder MTH, Islam AAA. A tale of a deep learning approach to image forgery detection, in 2018 5th International Conference on Networking, Systems and Security (NSysS). IEEE, 2018, pp.1–9. DOI
 43. Yao H, Xu M, Qiao T, Wu Y, Zheng N. Image Forgery Detection and Localization via a Reliability Fusion Map. *Sensors (Basel)* 2020;20:6668. DOI PubMed PMC
 44. Du M, Pentylala S, Li Y, Hu X. Towards generalizable deepfake detection with locality-aware autoencoder, in Proceedings of the 29th ACM International Conference on Information & Knowledge Management, 2020, pp. 325–334. DOI
 45. Thakur A, Jindal N. Machine learning based saliency algorithm for image forgery classification and localization, in 2018 First International Conference on Secure Cyber Computing and Communication (ICSCCC) IEEE, 2018, pp. 451–456. DOI
 46. Muhammad G, Al-hammadi MH, Hussain M, Bebis G. Image forgery detection using steerable pyramid transform and local binary pattern. *Machine Vision and Applications* 2014;25:985-95. DOI
 47. Warif NBA, Idris MYI, Wahab AWA, Ismail NN, Salleh R. A comprehensive evaluation procedure for copy-move forgery detection methods: results from a systematic review. *Multimed Tools Appl* 2022;81:15171-203. DOI
 48. Le-tien T, Phan-xuan H, Nguyen-chinh T, Do-tieu T; The authors are with the Department of Electrical and Electronics Engineering, University of Technology, National University of Ho Chi Minh city, Vietnam. Image forgery detection: a low computational-cost and effective data-driven model. *IJMLC* 2019;9:181-8. DOI
 49. Han J, Gevers T. MMD Based Discriminative Learning for Face Forgery Detection. In: Ishikawa H, Liu C, Pajdla T, Shi J, editors. *Computer Vision - ACCV 2020*. Cham: Springer International Publishing; 2021. pp. 121-36. DOI
 50. Aneja S, Nießner M. Generalized zero and few-shot transfer for facial forgery detection, arXiv preprint arXiv:2006.11863, 2020. DOI
 51. Bourouis S, Mashrgy MA, Bouguila N. Bayesian learning of finite generalized inverted Dirichlet mixtures: application to object classification and forgery detection. *Expert Systems with Applications* 2014;41:2329-36. DOI
 52. Cao S, Zou Q, Mao X, Wang Z. Metric learning for anti-compression facial forgery detection, arXiv preprint arXiv:2103.08397, 2021. DOI
 53. Srivastava V, Yadav SK. Frequency based edge-texture feature using Otsu's based enhanced local ternary pattern technique for digital image splicing detection. *Bulletin EEI* 2021;10:3147-55. DOI
 54. Zhang R, Ni J. A dense u-net with cross-layer intersection for detection and localization of image forgery, in Proc.2020 IEEE International Conference on Acoustics, Speech and Signal Processing (ICASSP), pp. 2982–2986. DOI
 55. Bottou L. On-line Learning and Stochastic Approximations. In: Saad D, editor. *On-Line Learning in Neural Networks*. Cambridge University Press; 2010. pp. 9-42. DOI
 56. Kingma D, Ba J. (2014). Adam: A Method for Stochastic Optimization. arXiv:1412.6980. DOI
 57. Loshchilov I, Hutter F. (2019). Decoupled Weight Decay Regularization. ICLR (Poster) 2019, arXiv:1711.05101v3. DOI
 58. "Torch.optim", torch.optim - PyTorch 1.11.0 documentation. [Online]. Available from: <https://pytorch.org/docs/stable/optim.html>[Last accessed on 9 Aug 2022]
 59. Tan M, Le QV. (2019). EfficientNet: Rethinking Model Scaling for Convolutional Neural Networks. ArXiv, abs/1905.11946. DOI
 60. Nam S, Ahn W, Yu I, Kwon M, Son M, Lee H. Deep Convolutional Neural Network for Identifying Seam-Carving Forgery. *IEEE Trans Circuits Syst Video Technol* 2021;31:3308-26. DOI
 61. Lu M, Niu SZ. (2019). Detection of Image Seam Carving Using a Novel Pattern, *Computational Intelligence and Neuroscience*, vol. 2019, Article ID 9492358, 15 pages, 2019. DOI

62. Senturk ZK, Akgun D. Seam carving based image resizing detection using hybrid features. *Tehnicki Vjesnik* 2017;24:1825-1832. DOI
63. Krizhevsky A, Sutskever I, Hinton GE. ImageNet classification with deep convolutional neural networks. In NIPS, pp. 1106–1114, 2012. DOI
64. Chollet F. Xception: Deep learning with depthwise separable convolutions, arXiv preprint, pp. 1610–02 357, 2017.